Science of the Total Environment 774 (2021) 145420

Contents lists available at ScienceDirect

Science of the Total Environment

journal homepage: www.elsevier.com/locate/scitotenv

Wetting/drying cycles increase arsenic bioaccessibility in mine-impacted sediments

Kevan P. O'Connor, Michaela Montgomery, Randy A. Rosales, Katherine K. Whiteman, Christopher S. Kim *

Schmid College of Science and Technology, Chapman University, One University Drive, Orange, CA 92866, United States of America

HIGHLIGHTS

- Arsenic exposure is a concern for residential areas adjacent to mine sites.
- Arsenic bioaccessibility in mine sediments is negatively correlated with rainfall.
- Rain events mobilize the most soluble/surface-bound arsenic from particles.
- Arsenic bioaccessibility gradually and progressively increases during dry periods.
- Humidity/temperature fluctuations enhance the formation of soluble arsenic phases.

GRAPHICAL ABSTRACT

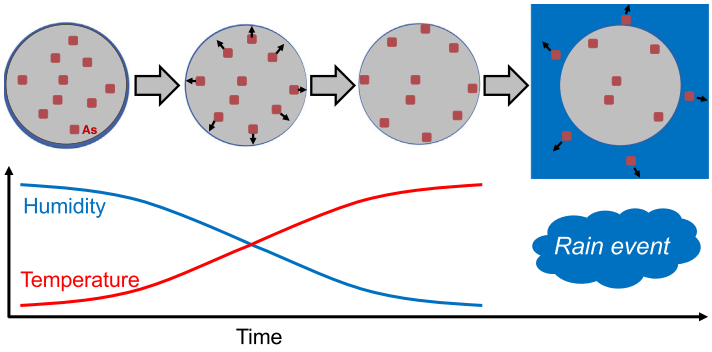

ARTICLE INFO

Article history:
Received 5 March 2020
Received in revised form 20 January 2021
Accepted 21 January 2021
Available online 26 January 2021

Editor: Mae Sexauer Gustin

Keywords:
Exposure
Mining
Rainwater
Solubility
Tailings

ABSTRACT

Physical and chemical weathering of arsenic-enriched mine wastes can lead to the mobilization and dispersal of contaminated sediments into surrounding (residential) areas. Additionally, seasonal effects during dry and rainy seasons affect contaminant bioaccessibility in ways that may significantly influence risk estimates of chronic arsenic exposure for residents living near mining sites. Rainwater-transported sediments from the Red Hill Mercury Mine in Tustin, California were collected monthly over a period of 25 months and the ingestible size fraction (≤250 μm) analyzed for bulk arsenic concentration (239 ± 149 mg/kg, n = 32, 114 to 678 mg/kg), assessed for arsenic bioaccessibility (11.2 ± 6.3%, n = 32, 2.7 to 24.9%), and compared with realtime rainfall data. Arsenic bioaccessibility was highly variable and strongly negatively correlated with cumulative rainfall over the preceding 40 days ($r^2 = 0.51$, $P < 0.001$). Controlled wetting/drying experiments and As speciation analyses demonstrated that this correlation primarily arose through the removal of soluble/surface-bound arsenic phases from sediments during rainwater exposure/transport, but also suggested the secondary formation of soluble arsenic phases resulting from diel humidity and temperature fluctuations during dry periods, which gradually increases the proportion of bioaccessible arsenic with time. These findings demonstrate significant seasonal variability in arsenic bioaccessibility and indicate that arsenic exposure risks through incidental ingestion in these and similar systems are highest following extended dry periods.

1. Introduction

Metal mining activities produce significant quantities of processed mine tailings and associated mine wastes containing elevated levels of trace metal(loid)s that would otherwise remain sequestered underground. For example, gold and silver mining throughout the state of

* Corresponding author.
E-mail address: cskim@chapman.edu (C.S. Kim).

https://doi.org/10.1016/j.scitotenv.2021.145420
0048-9697/

California have yielded millions of tons of mine wastes enriched in naturally-occurring arsenic (As), posing potential health threats to those exposed (Alpers et al., 2014; Kim et al., 2014; Kim et al., 2012; Kim et al., 2011; Tchounwou et al., 2003). When mining activities take place near current or future residential communities, occupants may be at increased risk for acute and/or chronic metal(loid) exposure via a number of mobilization and ingestion pathways (Martin et al., 2014; Rieuwerts et al., 2006).

Surface water, specifically rainwater, serves as a major mechanism for the transport of sediments when shearing forces produced by either raindrop impact or overland flow initiate particle detachment and movement (Bozhi et al., 2014; Croley, 1982). Due to the greater detachment capacity of intense rain events, rainfall rate and runoff sediment concentrations are commonly correlated (Proffitt et al., 1991). In areas of intermittent/low rainfall, the dominant fraction of sediment transport likely occurs during a few significant rain events rather than additively/continuously over time (Bennett, 1974).

The transport of As from mining-impacted regions during rain events is similarly dominated by particle-facilitated transport and As dissolution and transport in the dissolved phase (Kim et al., 2012). Other influences include past wetting and drying cycles (Shaoping et al., 2008) and the inverse relationship between particle size and As concentration observed in many mining environments (Kim et al., 2011). Additionally, extended dry periods may lead to preferential detachment and transport of fine-grained particles which, due to their increased surface area/mass ratio, are better able to adsorb and transport dissolved metal(loid)s during "first flush" rain events (Gupta and Saul, 1996; Lee et al., 2002; Wanielista and Yousef, 1993). Fine-grained particles travel greater distances from their source, become dispersed over wider areas, and are more likely to be incidentally ingested/inhaled than coarser particles, underscoring their importance in contributing to potential health threats when originating from mine-impacted environments (Kim et al., 2012).

Accordingly, the most significant risk of incidental exposure to metal (loid)-containing mine sediments should follow intense, sustained rain events that are preceded by extended dry periods (Gupta and Saul, 1996). However, a metal(loid)'s toxicity is not only a function of its absolute concentration in the environment, but also its potential solubility, bioaccessibility, and bioavailability (Reeder et al., 2006). The dynamics of repeated sediment wetting/drying cycles may induce changes in As speciation (defined here as the chemical species of As present and their relative proportions) that influence As bioaccessibility (the fraction of As released from the solid matrix, typically measured through *in vitro* methods) and As bioavailability (the fraction of As that reaches systemic circulation, typically measured through *in vivo* methods) continuously over time, rather than only during discrete rainfall events. Changes in As speciation can result from the dissolution and repartitioning of primary mineral phases into, or onto, secondary phases through a variety of mechanisms including adsorption, (co-)precipitation, and isomorphous substitution or structural incorporation (Foster et al., 2011; Foster and Kim, 2014).

An improved characterization of the seasonal effects of rainfall and wetting/drying cycles on the transport and bioaccessibility of As in mining-impacted sediments can enable more accurate exposure estimates and risk assessments for local communities. This study conducted rainwater runoff and sediment sampling at the Red Hill Mercury Mine in Tustin, Orange County, CA, followed by simulated gastric fluid extractions of collected sediments to calculate As exposure estimates and correlate them with historical rainfall records. Although this study is location-specific due to the frequency and variability of sampling demands, the conditions and context of mine-impacted sediments at the Red Hill Mine are comparable to those of As-bearing precious metal mines throughout the western US and elsewhere, and we anticipate that the relationships determined between wetting/drying events and As transport and mobility are relevant and transferable to a broad range of mine-impacted areas that experience seasonal weather variability. Specifically, we hypothesize that rainwater runoff contributes to As mobilization from mine sites into residential areas through both sediment transport and the dissolution of soluble As species, although the latter process has a secondary effect of diminishing As bioaccessibility in deposited sediments. Additionally, we hypothesize that extended dry periods between rain events are significant in enabling the gradual conversion of particle-associated As to more bioaccessible forms over time through diel fluxes in temperature and humidity.

2. Site background

Historical records report that cinnabar (HgS) deposits were first discovered at Red Hill in 1892; however, no production was officially recorded until 1927 to 1929 (Bradley, 1918; Bureau of Mines, 1965). At least 50,000 kg of mercury ore were extracted from the mine sporadically over the course of the following decade, after which time the mine shafts were sealed (Bradley, 1918; Bureau of Mines, 1965). Currently, more than two dozen residences share a property line with and are located downslope from the ~0.05 km^2 abandoned mine site (33°45′24″N 117°47′33″W, Fig. S1, Supplemental Information). Other studies have documented As contamination associated with mercury mines due to the elevated concentrations of As and other trace metal (loid)s during hydrothermal ore deposition processes (Larios et al., 2012b; Loredo et al., 1999). Additionally, As within roasted and processed mine tailings was determined through sequential extraction analysis to be more mobile than As associated with natural, undisturbed sources, indicating an increased risk of As distribution in the environment as a result of mining activity (Larios et al., 2012a).

The Red Hill Mine offers an unusual sampling scenario. The site is privately owned, preventing comprehensive spatial sampling; however, an impermeable asphalt driveway extends ~50 m from the south side of the mine hill downslope to the publicly accessible street below. The driveway channels rainfall runoff and mobilized sediments to the street, which then move downslope along the curb gutter perpendicular to the initial flow direction (Fig. S2). This assures that the dominant fraction of sediments collected at the base of the driveway above the curb was transported directly from the mine site by rainwater runoff.

3. Experimental method

3.1. Rainwater collection

Rainwater runoff was collected in real time during rain events from the driveway location as well as from a background site located in a concrete runoff trench 1.3 km northwest and 35 m higher in elevation than the mine. At each site, two 1 L HDPE bottles were pre-rinsed with rainwater and filled by capturing actively flowing runoff, then topped off with runoff collected with a 45-mL plastic pipette so no headspace remained in the bottles. Samples were stored in a 4 °C refrigerator within 1 h of collection. A total of 21 rainwater samples from the driveway location and 12 from the background location was collected between December 2012 and January 2015.

One liter of runoff from each sample collection was distributed into 50 mL Falcon tubes and centrifuged in a Beckman Coulter Avanti J-26S XPI centrifuge for 10 min at 2800 rpm to pellet the suspended sediment. The supernatants were filtered in a 1000 mL vacuum flask apparatus with an inline 0.45 μm non-sterile Fischer filter, changing the filter after every ~200 mL of supernatant. Samples collected prior to 11/30/12 were analyzed at the U.S. Geological Survey (Denver, CO) using either ICP-MS (ELAN DRC II Quadrupole ICP-MS) or ICP-OES (Perkin Elmer Optima 3000) for post-extraction concentrations of a suite of elements, including As, using USGS Method 37 (Azain, 2019). Subsequent collections were analyzed for metal and trace element concentrations at WECK Laboratories, using EPA method 200.7 (USEPA, 2001). Both analytical labs were supplied with lab deionized water and simulated gastric fluid sample blanks. Real-time rainfall rate data was obtained from

www.wunderground.com, station KCASANTA229, located 0.9 km west of the collection site. Where incomplete, additional rate data was obtained from stations KCATUSTI3 and KCASANTA279 located 3.4 km northwest and 1 km northeast from the collection site, respectively.

3.2. Sediment collection and characterization

A total of 32 sediment samples was collected from the driveway site and 27 samples from the background site between January 2013 and January 2015. Sample collection was attempted on a monthly basis (except where insufficient sample quantities precluded collection in certain months) and additionally within 24 h after significant rain events. Samples were collected using a pre-cleaned stainless steel gardening trowel and micro-spatula and transported to the laboratory in sealed plastic bags, where they were spread onto plastic trays and air-dried in a laboratory fume hood overnight. Sediment quantities varied significantly (450 ± 330 g, n = 32, 70–1200 g at the mine site; 400 ± 200 g, n = 27, 300–750 g at the background site). In order to separate the <250 μm "ingestible" size fraction (Plumlee and Ziegler, 2003), each sample was passed through a U.S. standardized test sieve no. 60 (250 μm) with a Tyler Industrial Products Model B Ro-Tap unit. Each sample was sieved continuously for 90 min. As the only sample preparation prior to further experimentation and analysis consisted of air-drying samples overnight and passing them through a physical sieving process, we expect that this minimal treatment would not induce significant changes in As speciation or bioaccessibility beyond those that would otherwise have occurred in situ.

Between 5 and 10 g of the unsieved bulk and ≤250 μm size fraction of each sample were sent for elemental concentration analysis to ALS Chemex, an international analytical testing services company located in Reno, NV that specializes in mineralogy and mining and mineral exploration. Aliquots of all received samples were pulverized using a ring mill prior to digestion and analysis such that >85% of the sample passed through a 75 μm (Tyler 200 mesh) screen. A 0.250 g sample of each aliquot was digested with $HClO_4$, HNO_3 and HF at 185 °C to near dryness and then further digested in a small volume of HCl. The solution was brought up to a final volume of 12.5 mL with 11% HCl, homogenized, and analyzed via ICP-AES (Varian Vista-PRO/Vista-725ES; 5 mg/kg As detection limit) for a suite of 49 elements.

3.3. EXAFS spectroscopy

The ≤250 μm size fraction of the following collected samples was selected for extended X-ray absorption fine structure (EXAFS) spectroscopy analysis: one sample collected directly from the mine hillside, several sediment samples representing a range of As bioaccessibility values collected from the driveway site, and aliquots of the same sediment samples following simulated gastric fluid exposure (described in the following section). Extended X-ray absorption fine structure (EXAFS) spectroscopy was conducted at beam lines 4–2 and 11–2 of the Stanford Synchrotron Radiation Lightsource. Arsenic K-edge EXAFS spectra were collected using Si (220), $\varphi = 90°$ monochromator crystals at room temperature in fluorescence mode with 32- or 100-element Ge detectors. Arsenic and aluminum foils were used for energy calibration and to attenuate sample matrix fluorescence, respectively. Multiple scans of each sample were averaged, background-subtracted, and fit using linear combination fitting over a k-range of 2–12.5 $Å^{-1}$ using the SixPack software program (Webb, 2005). Sample spectra were fitted using a database of previously-collected As model compound spectra with the "cycle fit" feature in the least squares fitting module of SixPack to determine the chemical speciation, or identities and proportions of As species, within each sample (Kim et al., 2013; Webb, 2005). Species were only included in final fitting results if they represented ≥10% of the total fit and caused the R-factor value to decline by ≥10%.

3.4. In vitro extractions

3.4.1. Simulated gastric fluid extractions

Simulated gastric fluid (SGF) extractions were performed using a modified version of the Solubility Bioaccessibility Research Consortium gastric phase extraction (SBRC-G), which has been extensively applied to assess As bioaccessibility in soils and sediments and validated against *in vivo* As bioavailability studies (Basta and Juhasz, 2014; Brattin et al., 2013; Ehlert et al., 2018; Juhasz et al., 2014a; Juhasz et al., 2014b; Juhasz et al., 2009). A 0.4 M glycine solution was adjusted to a pH of 1.5 ± 0.1 with concentrated UltraPurex nitric acid (in place of HCl in order to minimize interferences during solution analysis) at 37 °C. One-gram aliquots of the ≤250 μm size fraction from the site and background samples were separately exposed to 100 mL of SGF in 125 mL HDPE bottles and agitated at 190 rpm in a New Brunswick Scientific I2400 Incubator Shaker at 37 °C for 1 h. Suspensions were filtered using 0.45 μm non-sterile Fisher syringe filters to recover ~10 mL filtered aliquots, which were sent to Stanford University's Environmental Measurements Facility to measure dissolved As concentration via ICP-OES on a Thermo Scientific ICAP 6300 Duo View Spectrometer within 48 h of the extraction. All extractions were conducted in triplicate. Blank DI water samples and negative controls (SGF with no sediment added) were also analyzed in triplicate to correct for background As levels (Lee et al., 2006).

3.4.2. Pre-SGF sample wetting

In order to assess the water-soluble fraction of As prior to simulated gastric fluid extractions, selected sediment samples representing the range of As bioaccessibility at the site were exposed to DI water at a 0.5 g:13 mL ratio in 15 mL Falcon tubes. The tubes were vortexed, rotated at 8 rpm for 1 h in a Barnstead Thermolync Labquake Shaker/Rotisserie at room temperature, centrifuged at 2800 rpm for 10 min, and decanted into 50 mL Falcon tubes. The sediments were then re-exposed, centrifuged, and decanted twice more before being subject to SGF extractions using the aforementioned protocol at a 1.0 g:100 mL solid:solution ratio.

3.4.3. Sample wetting/drying under ambient conditions

Samples from the mine site and the designated background location collected on 3/3/2014 were sieved to the ≤250 μm size fraction, with each sample then divided into five 1.5 g subsamples. The pair of samples was chosen because of the relatively high initial As concentration (449 mg/kg) at the mine site and because that date was preceded by the largest local rain event to take place over the duration of the study (28 mm/day). The subsamples were placed on individual watch glasses covered with perforated clear plastic shields to allow exposure to ambient air, temperature, humidity, and light conditions while minimizing dust contamination and placed on the roof of a 4-story building on the Chapman University campus, ~7.5 km northwest of the Red Hill Mine.

Each week for the subsequent four weeks, one of the mine site and background subsamples underwent the water rinse described above before being returned to the roof. At the conclusion of this period, all samples were exposed in triplicate to the aforementioned SGF extraction with a 1.0 g:100 mL suspension ratio, representing 0, 7, 14 or 21 days since water exposure, with one subsample that had been exposed to the ambient atmosphere for 28 days without a water rinse. No rain events were recorded during this time period, but temperature ranged from 12 to 32 °C (avg. 21 °C) and humidity ranged from 12 to 99% (avg. 78%) according to www.wunderground.com using station KCAORANG22, located 1 km southeast of the experimental location.

3.5. Arsenic bioaccessibility, intake, exposure, and speciation calculations

In vitro As bioaccessibility was calculated by dividing the mass of As in the supernatant of the simulated gastric fluid extractions by the initial mass of As present in the solid sample fraction (Eq. (1)):

$$\textit{In Vitro}\ \text{As Bioaccessibility (IVBA)}\ (\%) = \frac{[\text{As}]_{\text{SGF}}\left(\frac{\text{mg}}{\text{L}}\right) \times \text{volume}_{\text{SGF}}(\text{L})}{[\text{As}]_{\text{solid}}\left(\frac{\text{mg}}{\text{kg}}\right) \times \text{mass}_{\text{solid}}\ (\text{kg})} \quad (1)$$

Arsenic intake was calculated assuming body weights for adults and children of 70 and 35 kg, respectively (Davis and Mirick, 2006; Hogan et al., 1998; Martin et al., 2014), and incidental soil ingestion rates of 100 and 200 mg/day, respectively (Lee et al., 2006; USEPA, 2017) (Eq. (2)).

$$\text{Arsenic Intake}\left(\frac{\frac{\mu\text{g}}{\text{kg}}}{\text{day}}\right) = \text{Incidental Soil Ingestion}\left(\frac{\text{mg}}{\text{day}}\right) \times \frac{1\ \text{kg}}{1 \times 10^6\ \text{mg}} \times \frac{[\text{As}]_{\text{solid}}\ (\text{mg/kg})}{\text{Body Weight}\ (\text{kg})} \times \frac{1000\ \mu\text{g}}{1\ \text{mg}} \quad (2)$$

Arsenic exposure calculations effectively moderate As intake rates by accounting for As bioaccessibility, determined in this study by SGF extraction (Eq. (1)). That is, while As intake represents the total potential quantity of As ingested, As exposure represents the (soluble) quantity of As that can be potentially mobilized in the body and enter systemic circulation (Eq. (3)).

$$\text{Arsenic Exposure}\left(\frac{\frac{\mu\text{g}}{\text{kg}}}{\text{day}}\right) = \text{Arsenic Intake}\left(\frac{\frac{\mu\text{g}}{\text{kg}}}{\text{day}}\right) \times \text{IVBA}\ (\%) \quad (3)$$

To assess changes in As speciation pre- and post-SGF exposure, it is necessary to account for the sample's initial As concentration and bioaccessibility, as EXAFS speciation analysis yields proportions of As species as a fraction of all As present in the given sample; thus, comparing these percentages directly can give misleading results regarding a particular species' absolute change in abundance. Accordingly, As speciation must be converted from percentage to mass units as follows:

Pre-SGF speciation:

$$\text{Concentration of As species } i\ (\text{mg/kg}) = [\text{As}]_{\text{solid}}\ (\text{mg/kg}) \times \text{f}_i \quad (4)$$

Post-SGF speciation:

$$\text{Concentration of As species } i\ (\text{mg/kg}) = [\text{As}]_{\text{solid}} \times (1 - \text{IVBA}\ (\%)) \times \text{f}_i \quad (5)$$

where f_i = fraction of As species i as determined by EXAFS linear combination fitting analysis.

4. Results and discussion

4.1. Arsenic concentration in rainwater runoff

Collected rainwater runoff samples from the mine site were significantly elevated in both total As (168 ± 141 μg/L, n = 21, 33–531 μg/L) and dissolved As (134 ± 138 μg/L, n = 21, 23–506 μg/L) compared to background rainwater collections (total As: 4 ± 3 μg/L, n = 12, <1–9.1 μg/L; dissolved As: 3 ± 2 μg/L, n = 12, <1–5.1 μg/L) (Table S1, Supporting Information) and to the EPA's Maximum Contaminant Level (MCL) for arsenic in drinking water of 10 μg/L (USEPA, 2001). The elevated As concentrations in the filtered samples from the mine site suggest that rainwater exposure facilitated the dissolution of soluble As phases and transport of dissolved As in runoff.

The proportion of undissolved (i.e., particulate) As in the mine site rainwater samples varied considerably (26 ± 23%, n = 18, 0 to 80%) and is moderately correlated ($r^2 = 0.25$, $P = 0.047$) with rainfall rate at the time of collection (Fig. 1a). This is comparable to the correlation between solid As concentration and rainfall rate (Fig. 1b, $r^2 = 0.25$, $P = 0.047$) and considerably greater than that between rainfall rate and either dissolved or total As concentration (Fig. 1c, d, $r^2 = 0.02$ and 0.00, respectively (trendlines not shown), $P > 0.05$ for both), indicating that As-bearing sediments from the mine site are actively transported in surface water runoff during rain events. However, there was likely wide variability in sediment mobilization, possibly even during a single rain event (e.g., an initial pulse of sediment followed by much less particle mobilization with continued rainfall). Additionally, differences between measured rainfall rates at the weather stations (located 0.9–3.4 km away) and rainfall rates at the site during sampling, or potential inconsistencies in rainwater runoff sampling over time, could have further impaired the strength of this correlation.

4.2. Arsenic concentration in sediments

As concentrations within the ingestible size fraction of the collected mine site sediments (239 ± 149 mg/kg, n = 32, 114 to 678 mg/kg) were enriched by as much as 471% (average 125%) over their corresponding bulk As concentrations (142 ± 132 mg/kg, n = 32, 27 to 567 mg/kg) and over an order of magnitude higher than the background samples (10 ± 4 mg/kg, n = 27, 5 to 17 mg/kg) (Table S2, Supporting Information) and the continental average As concentration in surface soils (6.4 mg/kg) (Smith et al., 2013). Interestingly, mercury concentrations were relatively low across the ingestible size fraction of the collected mine site sediment samples (23 ± 17 mg/kg, n = 32, 5 to 91 mg/kg), despite the history of the site as a mercury ore source. All available geochemical data on mine site sediments and background samples (both bulk and sieved) are available in the Supporting Information.

4.3. Arsenic bioaccessibility

Arsenic bioaccessibility, as determined by simulated gastric fluid extractions, ranged from 2.7% to 24.9% (11.2 ± 6.3%, n = 32) among all ≤250 μm sieved sediment samples (Table S2, Supporting Information). This wide range is representative of other studies measuring arsenic bioaccessibility in mine-impacted soils and associated materials, which report *in vitro* arsenic bioaccessibility values ranging from ~1% to >50% (Juhasz et al., 2014b; Meunier et al., 2011; Meunier et al., 2010; Toujaguez et al., 2013; Whitacre et al., 2017). Such variability is due to a complex combination of factors including but not limited to spatial distribution of As (e.g. from fully-encapsulated As to within or coating particle grains), chemical speciation of As (e.g. crystalline, co-precipitate, amorphous, sorbed, phases), and As solubility of such phases under different extraction conditions (e.g. water, *in vitro* bioaccessibility assays). One key distinction of the current study, however, is that the range of As bioaccessibility was observed among samples collected at a single individual site over time as opposed to a number of locations, suggesting dynamic processes that influence As mobility and bioaccessibility *in situ*.

Arsenic bioaccessibility and daily rainfall were inversely related with one another (Fig. 2). For example, bioaccessibility generally increased from <5% in January 2013 to 25% in February 2014; this timeframe corresponded with relatively low rainfall due to California's drought-like conditions at the time until a single large rain event at the end of February 2014 resulted in a rapid decrease or "reset" in As bioaccessibility. Similarly, the subsequent dry months that followed correspond with continued increases in bioaccessibility until the onset of the rainy season in November 2014.

Due to the asynchronous times at which As bioaccessibility and rainfall were measured as well as the likelihood that cumulative instead of daily rainfall would correlate more significantly with bioaccessibility, we conducted an analysis of linear correlation coefficients for log-transformed As bioaccessibility, sediment As concentration, and As exposure against cumulative rainfall over 1–120 day timeframes (Fig. 3). The analysis shows that the cumulative rainfall over the 40 days prior to sediment collection was most strongly correlated with the As

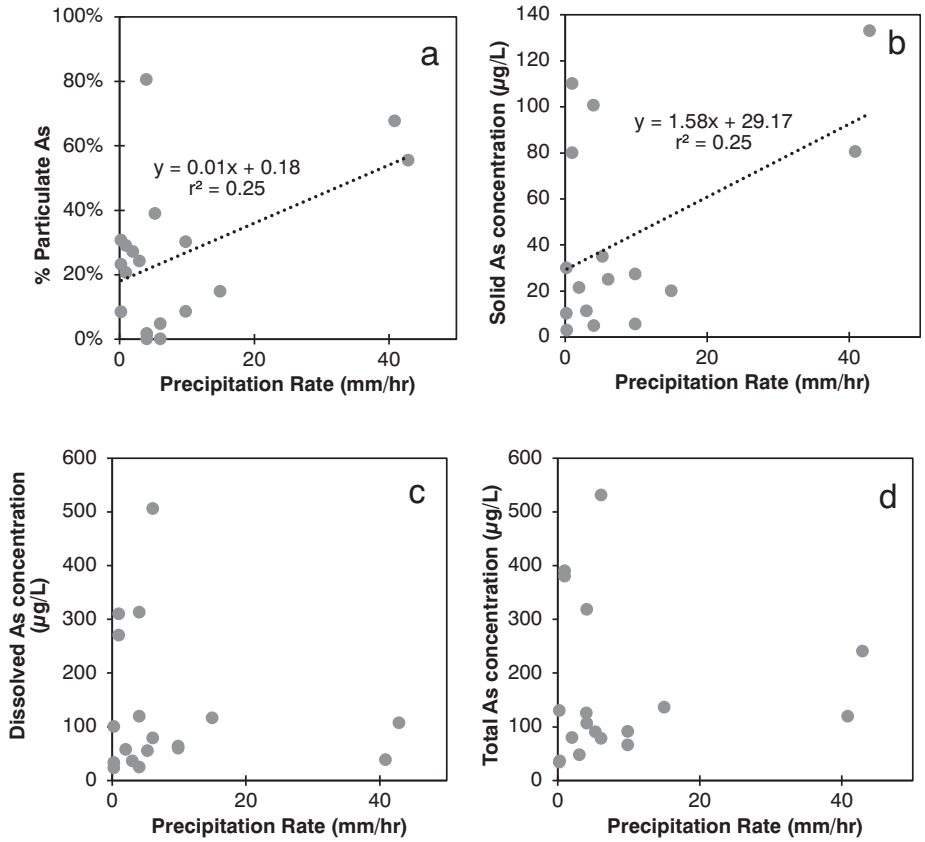

Fig. 1. Precipitation rate at the time of sample collection plotted against a) percentage of particulate (undissolved) arsenic ($P = 0.047$), b) arsenic concentration of solids ($P = 0.047$), c) percentage of dissolved arsenic ($P > 0.05$), and d) percentage of dissolved arsenic in rainwater runoff samples ($P > 0.05$) in rainwater runoff samples. Samples where precipitation rates were not recorded or where filtered concentrations (slightly) exceeded unfiltered concentrations were not included in figure.

bioaccessibility (and thus arsenic exposure) of the sediment (Fig. 4; $r^2 = 0.51$ using an exponential regression, $P < 0.001$ using log-transformed, linearized data). This correlation may be explained in at least two possible ways: 1) rainwater dissolved and removed the most soluble As species from the solid matrix, resulting in reduced As bioaccessibility in sediments during and immediately following rain events; and 2) gradual formation of secondary As-bearing phases at particle surfaces, or migration of As towards particle surfaces, during dry periods promoted increased As bioaccessibility. Such secondary As phase formation may occur through very gradual dissolution/

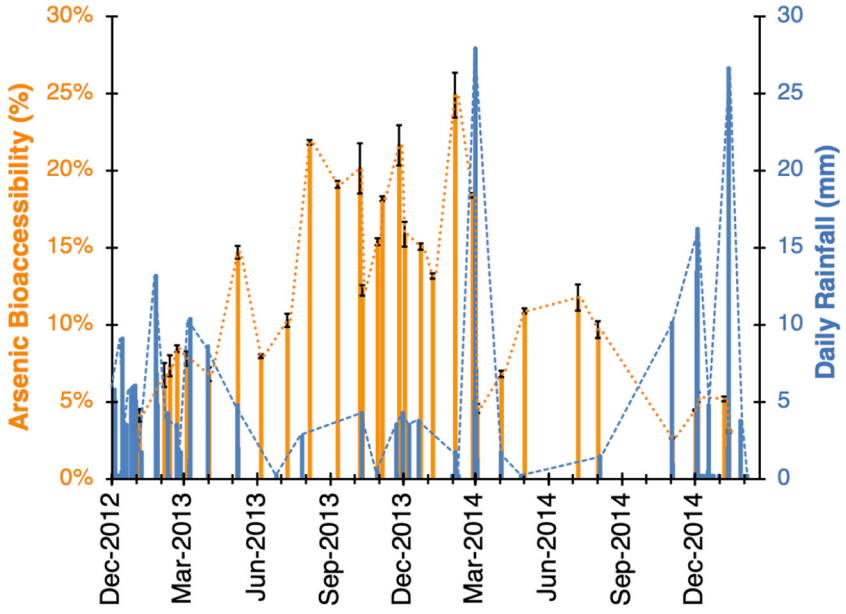

Fig. 2. Arsenic bioaccessibility of mine-impacted sediments (orange bars) and daily rainfall totals in millimeters (blue bars) over the sampling period December 2012–February 2015. Dashed/dotted lines are provided as visual aids. (For interpretation of the references to colour in this figure legend, the reader is referred to the web version of this article.)

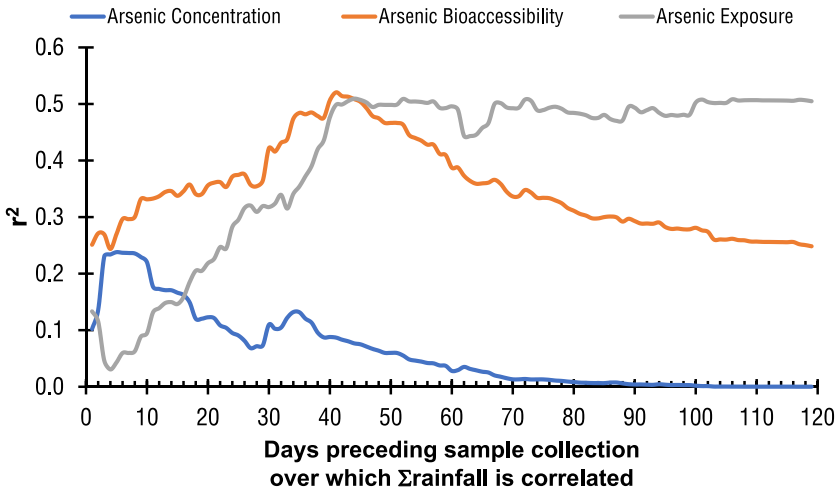

Fig. 3. Linear correlation coefficients between cumulative rainfall over variable time periods (1–120 days) preceding sample collection and sediment arsenic concentration (blue), arsenic bioaccessibility (orange), and arsenic exposure (gray). (For interpretation of the references to colour in this figure legend, the reader is referred to the web version of this article.)

reprecipitation processes occurring as the result of diel fluxes in temperature and humidity, as has been documented by the production of soluble metal sulfate efflorescent salt phases in other mining environments (Meza-Figueroa et al., 2009; Nordstrom and Alpers, 1999; Sobron et al., 2009; Valente et al., 2013).

It is notable that the As concentration in collected sediments reached a maximum correlation with cumulative rainfall after a 5-day period, while the As bioaccessibility of the sediments was dependent on a longer timeframe of cumulative rainfall (peaking at 40 days but persisting out to and beyond 120 days) (Figs. 3, S3, Supporting Information). This is likely because As sediment concentration is highly dependent on the transport of sediments off of Red Hill during more intense, short-term rain events. In contrast, the dependence of As bioaccessibility on longer timeframes may be associated with the removal by subsequent/multiple rain events of bioaccessible phases produced through diel variations in temperature and humidity.

4.4. Effect of water exposure/drying time on As bioaccessibility

Rinsing of selected runoff sediments immediately prior to SGF extractions resulted in a 13–39% relative decrease (1.3–4.1% absolute decrease) in As bioaccessibility (Fig. 5, Table S3, Supporting Information). Additionally, a slight positive relationship can be observed between post-wetting drying time and As released through SGF in the selected mine site sediment sample (Fig. S4, Supporting Information), with a 36% relative increase in bioaccessibility observed over a 4-week timeframe relative to the background sample. This difference indicates that airborne deposition of allochthonous material onto the sediment sample did not contribute significantly to its apparent increase in As bioaccessibility with time. However, the observed trend in the mine-impacted sediment sample is not statistically significant except when comparing the unrinsed sample to the samples rinsed 0 days ($P = 0.024$) and 7 days ($P = 0.019$) prior to SGF extraction. Examination over longer timeframes and in more controlled humidity/temperature conditions may more conclusively demonstrate the extent to which As bioaccessibility increases during dry time periods.

Together, however, these wetting/drying experimental results confirm that rain events rapidly remove the more bioaccessible (soluble) As phases in deposited sediments, thus reducing potential As exposure upon ingestion, and suggest that during subsequent dry periods As bioaccessibility can continuously increase in sediments over time, perhaps due to the (re)formation of soluble secondary As phases. The latter observation is consistent with the mechanism of stoichiometric precipitation in which supersaturation achieved through evaporation of moisture leads to the formation of secondary phases (Foster et al., 2011), and supports observations within the field data indicating an

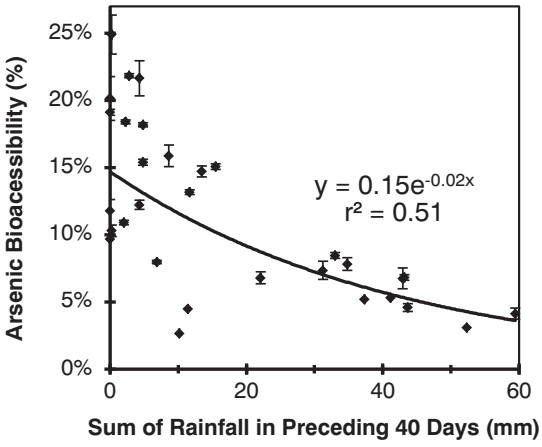

Fig. 4. Arsenic bioaccessibility of deposited sediments as a function of cumulative rainfall in the 40-day period preceding sample collection ($P < 0.001$).

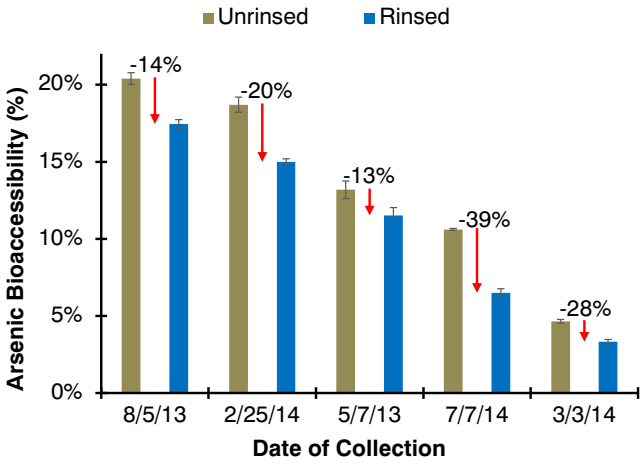

Fig. 5. Effect of simulated rainwater exposure on arsenic bioaccessibility of the ingestible size fraction (≤250 μm particle diameter) of collected sediments.

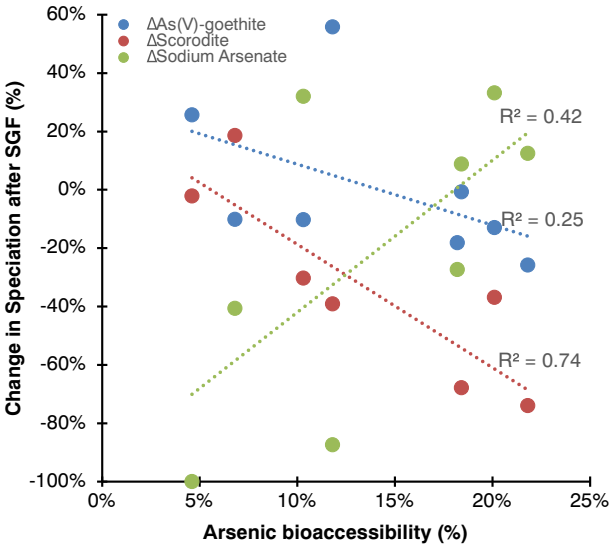

Fig. 6. Changes in speciation of As phases determined by EXAFS spectroscopy after simulated gastric fluid (SGF) extraction plotted against total arsenic bioaccessibility ($P = 0.01$, 0.08, and 0.20 for scorodite, Na-arsenate, and As(V) sorbed to goethite, respectively).

increase in bioaccessibility during extended dry periods (Figs. 2, 4). Diel fluctuations in humidity could contribute daily to this process; over the 25-month period during which samples were collected, the area experienced average humidity highs and lows of 88% and 42%, respectively.

4.5. As speciation and effects of simulated gastric fluid extraction on speciation

EXAFS spectroscopic analysis indicates essentially identical As speciation in the runoff-transported sediments and the mine hill itself, with linear combination fitting of the EXAFS spectra identifying ferric arsenate (65% and 57% respectively) and As(V) sorbed to iron oxyhydroxide species (37% and 33% respectively) in both samples (Fig. S5, Supporting Information). These speciation results support the mine hill as the primary source of the runoff sediment collected at the bottom of the Red Hill driveway and indicate that no substantial changes in speciation occurred during transport.

Analysis of the selected sediment samples for which As speciation was determined pre- and post-SGF extraction using EXAFS spectroscopy reveals species-dependent relationships between total As bioaccessibility and changes in As speciation (Fig. 6, Table S4, Supporting Information). Specifically, increasing bioaccessibility is correlated with greater removal of species identified as scorodite ($FeAsO_4$) and As (V) sorbed to goethite (a-FeOOH), and with an increased abundance of a species identified as sodium arsenate (Na_3AsO_4, identification of which may be a proxy for a range of more crystalline arsenate phases, e.g., Mg-arsenate, Ca-arsenate, Fe-arsenate). This suggests that the former species are more readily removed from the solid phase upon simulated ingestion due to a combination of higher solubility and greater abundance at particle surfaces, while secondary precipitation of crystalline arsenate phases may occur in samples with greater As bioaccessibility and thus higher concentrations of dissolved arsenic available for reprecipitation. Other studies similarly suggest widely varying solubilities of arsenic species in both synthetic and mine waste materials (Drahota et al., 2014; Paktunc and Bruggeman, 2010; Paktunc et al., 2008). It should be noted that the trends described are statistically strongest for scorodite ($r^2 = 0.74$, $P = 0.01$) and considerably less so for Na-arsenate and As(V) sorbed to goethite ($r^2 = 0.42$ and 0.25, $P = 0.08$ and 0.20, respectively); however, these represent the first known spectroscopic results to demonstrate differential changes in speciation as the result of simulated ingestion and underscore the importance of speciation in predicting As bioaccessibility and potential bioavailability.

Our prior EXAFS studies concluded that the presence of As(V) sorbed to iron oxyhydroxides is more common among sediments that have been transported compared to native ore or mine tailings samples (Kim et al., 2013), indicating that the dissolution of crystalline arsenic species from source material was followed by the subsequent sorption of As to iron phases. Similarly, (amorphous) iron oxides have been identified in other studies as a potential sink for As and a control for As mobility and availability in agricultural soils (Liu et al., 2015; Liu et al., 2010; Yu et al., 2016) under typical aqueous geochemical conditions. The findings reported here suggest that when exposed to more

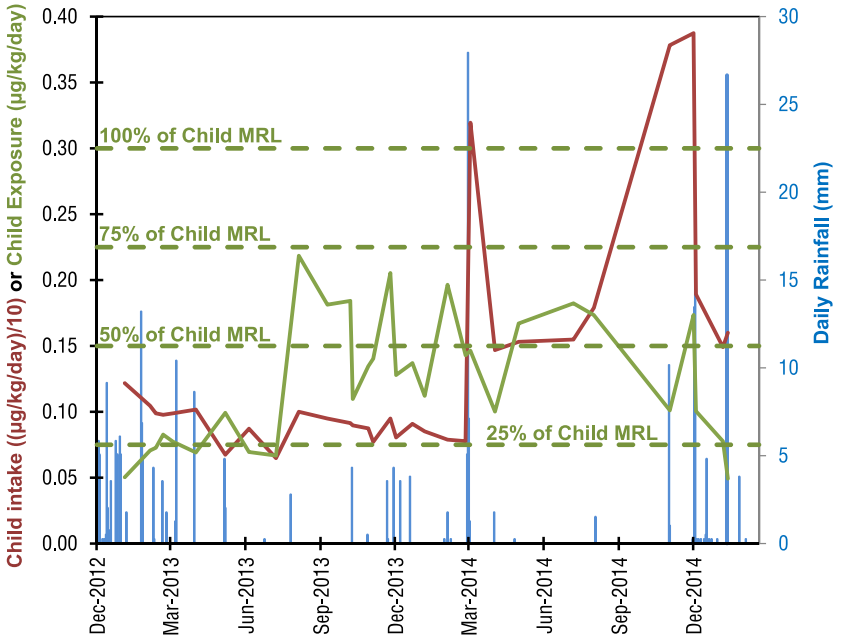

Fig. 7. Child arsenic intake (red line), child arsenic exposure (green line), and daily rainfall (blue bars) over the sampling period December 2012–February 2015. Dashed lines indicating percentages of the chronic arsenic minimal risk level (MRL) are provided for reference.

aggressive extractants such as simulated gastric fluid, such sorbed arsenic species can be considerably more mobile.

4.6. Arsenic intake and exposure trends

The correlation between rainfall and particulate As mobilization/deposition (Fig. 1a), though modest, would imply that the potential for incidental As intake is greatest immediately following intense rain events. However, As exposure is also strongly dependent on As bioaccessibility, which is negatively associated with rainfall quantity (Fig. 2). Accordingly, when plotted as a function of time/rainfall and using children as the base population due to their greater exposure risk, potential As intake and exposure rates show noticeably divergent trends (Fig. 7). Large rain events corresponded with significant increases in As intake (e.g., Mar. 2014, Dec. 2014), while sustained dry periods corresponded with elevated As exposure (e.g., Aug. 2013–Feb. 2014, Apr.–Nov. 2014). Potential child As exposure was negatively correlated with the sum of rainfall in the preceding 40-day period (Fig. 8) ($r^2 = 0.48$ using an exponential regression, $P < 0.001$ using log-transformed, linearized data). Therefore, although larger precipitation rates generally result in higher quantities of sediment as well as As sediment concentrations, the relationship between preceding rainfall totals and bioaccessibility has a much more significant effect on estimated As exposure. This further corroborates the conclusions from the wetting/drying experiments, which identify both rainfall events and dry period duration as contributing factors to As bioaccessibility.

Exposure risk is evaluated using minimum risk levels (MRLs) that propose the lowest daily human exposure (μg/kg/day) to a substance at which adverse, non-cancer health effects are appreciably observed for a given exposure duration. The U.S. Department of Health's Agency for Toxic Substances and Disease Registry (ATSDR) has established the As MRL for acute (≤14 days) and chronic (≥1 year) exposure scenarios at 5.0 and 0.3 μg As/kg/day, respectively (ATSDR, 2008). Although child exposure calculations show that the chronic MRL was not exceeded over the timeframe investigated (Fig. 7, 41 ± 17% of MRL, n = 31, 17%–73%), the effects of sustained dry periods on dust fluxes and potential ingestion/exposure rates may increase over time, particularly if extended drought conditions (e.g., resulting from climate change effects) persist in the future.

The inverse relationship between topsoil moisture content and dust flux at the near-ground level (Offer and Goossens, 2004) suggests that as dry conditions continue, dust mobilization in urbanized regions will increase due to disturbances by wind, cars, construction, and foot traffic. Therefore, during drought conditions such as those recently and frequently experienced throughout the state of California, the current dust ingestion rates used in risk calculations may prove to be both insufficiently conservative and seasonably variable. Furthermore, the amount of rainfall received during a wet season affects the dust activity of the following dry season such that wet seasons with little rainfall are typically followed by dry seasons with high dust activity (Offer and Goossens, 2001). The combination of elevated dust activity, increased dust ingestion, and high As bioaccessibility during dry periods further suggests that As exposure risks via the incidental ingestion pathway could eventually exceed MRLs in a progressively warmer and drier environment.

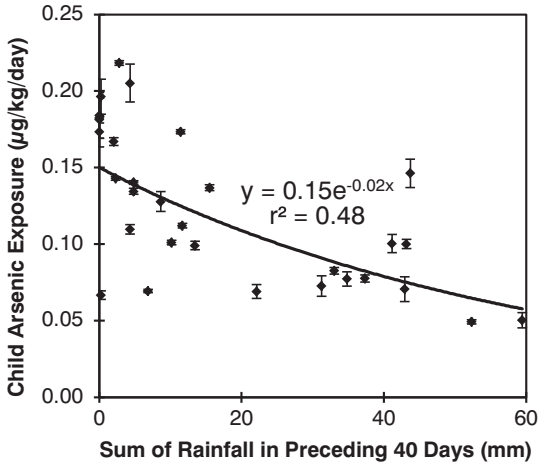

Fig. 8. Child arsenic exposure as a function of cumulative rainfall in the 40-day period preceding sample collection ($P < 0.001$).

5. Conclusions

The physical and chemical weathering of As-bearing and, by extension, other metal(loid)-enriched sediments over time can influence the mobilization, bioaccessibility, and exposure of potentially harmful elements in complex ways. Rainfall events and cumulative rainfall amounts readily transported As-bearing particles and enabled the release of more soluble and/or surface-bound As species into solution, thus lowering As bioaccessibility in the resulting deposited sediments. However, these sediments are not unreactive, inert and static substrates, but rather dynamic materials where As bioaccessibility can both diminish quickly during rain events and gradually increase during dry periods due to gentle daily fluctuations in humidity and temperature. Accordingly, estimations of As exposure risks in communities proximate to As-enriched sediments and mine wastes should account for (changes in) As bioaccessibility, As speciation, and regional/temporal weather trends that influence the wetting/drying cycles to which As-bearing materials are exposed.

CRediT authorship contribution statement

Kevan P. O'Connor: Formal analysis, Investigation, Methodology, Visualization, Writing – original draft. **Michaela Montgomery:** Formal analysis, Visualization, Writing – review & editing. **Randy A. Rosales:** Formal analysis, Investigation, Methodology, Visualization. **Katherine K. Whiteman:** Formal analysis, Investigation, Visualization. **Christopher S. Kim:** Conceptualization, Funding acquisition, Methodology, Project administration, Supervision, Validation, Writing – review & editing.

Declaration of competing interest

The authors declare that they have no known competing financial interests or personal relationships that could have appeared to influence the work reported in this paper.

Acknowledgements

This work was funded by NSF-CAREER Award No. 0847811. Use of the Stanford Synchrotron Radiation Lightsource, SLAC National Accelerator Laboratory, is supported by the U.S. Department of Energy, Office of Science, Office of Basic Energy Sciences under Contract No. DE-AC02-76SF00515. The assistance of SSRL staff scientists Sam Webb and Ryan Davis in EXAFS data collection was greatly appreciated. The authors also wish to thank the many past Kim Environmental Geochemistry Laboratory members who participated in field sampling and lab analyses.

Appendix A. Supplementary data

Supplementary data to this article can be found online at https://doi.org/10.1016/j.scitotenv.2021.145420.

References

Alpers, C.N., Myers, P.A., Millsap, D., Regnier, T.B., 2014. Arsenic Associated With Historical Gold Mining in the Sierra Nevada Foothills: Case Study and Field Trip Guide for Empire Mine State Historic Park, California. 79. Mineralogical Society of America, Reviews in Mineralogy & Geochemistry. pp. 553–587.

ATSDR, 2008. Evaluation of Soil Arsenic Concentrations at the Rand Historical Mining Complex, Kelly Mine Site, Red Mountain, San Bernardino County, California. U. S. Department of Health and Human Services, Atlanta, Georgia.
Azain, J., 2019. Method 37 - Inductively Coupled Plasma-Optical Emission Spectrometry-Mass Spectrometry (ICP-OES-MS) Water.
Basta, N.T., Juhasz, A., 2014. Using in vivo bioavailability and/or in vitro gastrointestinal bioaccessibility testing to adjust human exposure to arsenic from soil ingestion. In: Bowell, R.J., Alpers, C.N., Jamieson, H.E., Nordstrom, D.K., Majzlan, J. (Eds.), Arsenic: Environmental Geochemistry, Mineralogy, and Microbiology. 79, pp. 451–472.
Bennett, J.P., 1974. Concepts of mathematical-modeling of sediment yield. Water Resour. Res. 10, 485–492.
Bozhi, R., Kejia, L., Hongpu, M., Hongtao, Z., Xie, Z., 2014. SWAT model for analysis of pollution load of manganese in rainwater runoff in a manganese mine. J. Chem. Pharm. Res. 6, 1922–1928.
Bradley, W.W., 1918. In: Bureau CSM (Ed.), Quicksilver Resources of California With a Section on Metallurgy and Ore-Dressing. 78. California State Mining Bureau, San Francisco, CA, p. 389.
Brattin, W., Drexler, J., Lowney, Y., Griffin, S., Diamond, G., Woodbury, L., 2013. An in vitro method for estimation of arsenic relative bioavailability in soil. Journal of Toxicology and Environmental Health-Part a-Current Issues 76, 458–478.
Bureau of Mines, 1965. Mercury Potential of the United States. United States Department of the Interior, p. 375.
Croley, T.E., 1982. Unsteady overland sedimentation. J. Hydrol. 56, 325–346.
Davis, S., Mirick, D.K., 2006. Soil ingestion in children and adults in the same family. Journal of Exposure Science & Environmental Epidemiology 16, 63–75.
Drahota, P., Grosslova, Z., Kindlova, H., 2014. Selectivity assessment of an arsenic sequential extraction procedure for evaluating mobility in mine wastes. Anal. Chim. Acta 839, 34–43.
Ehlert, K., Mikutta, C., Jin, Y., Kretzschmar, R., 2018. Mineralogical controls on the bioaccessibility of arsenic in Fe(III)-As(V) coprecipitates. Environ. Sci. Technol. 52, 616–627.
Foster, A.L., Kim, C.S., 2014. Arsenic speciation in solids using X-ray absorption spectroscopy. In: Bowell, R.J., Alpers, C.N., Jamieson, H.E., Nordstrom, D.K., Majzlan, J. (Eds.), Arsenic: Environmental Geochemistry, Mineralogy, and Microbiology. 79, pp. 257–369.
Foster, A.L., Ashley, R.P., Rytuba, J.J., 2011. Arsenic species in weathering mine tailings and biogenic solids at the Lava Cap Mine Superfund Site, Nevada City, CA. Geochem. Trans. 12, 1–21.
Gupta, K., Saul, A.J., 1996. Specific relationships for the first flush load in combined sewer flows. Water Res. 30, 1244–1252.
Hogan, K., Marcus, A., Smith, R., White, P., 1998. Integrated exposure uptake biokinetic model for lead in children: empirical comparisons with epidemiologic data. Environ. Health Perspect. Suppl. 106, 1557.
Juhasz, A.L., Weber, J., Smith, E., Naidu, R., Rees, M., Rofe, A., et al., 2009. Assessment of four commonly employed in vitro arsenic bioaccessibility assays for predicting in vivo relative arsenic bioavailability in contaminated soils. Environ. Sci. Technol. 43, 9487–9494.
Juhasz, A.L., Herde, P., Herde, C., Boland, J., Smith, E., 2014a. Validation of the predictive capabilities of the Sbrc-G in vitro assay for estimating arsenic relative bioavailability in contaminated soils. Environ. Sci. Technol. 48, 12962–12969.
Juhasz, A.L., Smith, E., Nelson, C., Thomas, D.J., Bradham, K., 2014b. Variability associated with as in vivo-in vitro correlations when using different bioaccessibility methodologies. Environ. Sci. Technol. 48, 11646–11653.
Kim, C.S., Wilson, K.M., Rytuba, J.J., 2011. Particle-size dependence on metal(loid) distributions in mine wastes: implications for water contamination and human exposure. Appl. Geochem. 26, 484–495.
Kim, C.S., Stack, D.H., Rytuba, J.J., 2012. Fluvial transport and surface enrichment of arsenic in semi-arid mining regions: examples from the Mojave Desert, California. J. Environ. Monit. 14, 1798–1813.
Kim, C.S., Chi, C., Miller, S.R., Rosales, R.A., Sugihara, E.S., Akau, J., et al., 2013. (Micro)spectroscopic analyses of particle size dependence on arsenic distribution and speciation in mine wastes. Environ. Sci. Technol. 47, 8164–8171.
Kim, C.S., Anthony, T.L., Goldstein, D., Rytuba, J.J., 2014. Windborne transport and surface enrichment of arsenic in semi-arid mining regions: examples from the Mojave Desert, California. Aeolian Res. 14, 85–96.
Larios, R., Fernández-Martínez, R., Álvarez, R., Rucandio, I., 2012a. Arsenic pollution and fractionation in sediments and mine waste samples from different mine sites. Sci. Total Environ. 431, 426–435.
Larios, R., Fernandez-Martinez, R., Silva, V., Loredo, J., Rucandio, I., 2012b. Arsenic contamination and speciation in surrounding waters of three old cinnabar mines. J. Environ. Monit. 14, 531–542.
Lee, J.H., Bang, K.W., Ketchum, L.H., Choe, J.S., Yu, M.J., 2002. First flush analysis of urban storm runoff. Sci. Total Environ. 293, 163–175.
Lee, S.W., Lee, B.T., Kim, J.Y., Kim, K.W., Lee, J.S., 2006. Human risk assessment for heavy metals and as contamination in the abandoned metal mine areas, Korea. Environ. Monit. Assess. 119, 233–244.
Liu, C.-p., Luo, C.-l., Gao, Y., Li, F.-b., Lin, L.-w., Wu, C.-a., et al., 2010. Arsenic contamination and potential health risk implications at an abandoned tungsten mine, southern China. Environ. Pollut. 158, 820–826.
Liu, C., Yu, H.-Y., Liu, C., Li, F., Xu, X., Wang, Q., 2015. Arsenic availability in rice from a mining area: is amorphous iron oxide-bound arsenic a source or sink? Environ. Pollut. 199, 95–101.
Loredo, J., Ordonez, A., Gallego, J.R., Baldo, C., Garcia-Iglesias, J., 1999. Geochemical characterisation of mercury mining spoil heaps in the area of Mieres (Asturias, northern Spain). J. Geochem. Explor. 67, 377–390.
Martin, R., Dowling, K., Pearce, D., Sillitoe, J., Florentine, S., 2014. Health effects associated with inhalation of airborne arsenic arising from mining operations. Geosciences 4 (2076–3263), 128–175.
Meunier, L., Walker, S.R., Wragg, J., Parsons, M.B., Koch, I., Jamieson, H.E., et al., 2010. Effects of soil composition and mineralogy on the bioaccessibility of arsenic from tailings and soil in gold mine districts of Nova Scotia. Environ. Sci. Technol. 44, 2667–2674.
Meunier, L., Koch, I., Reimer, K.J., 2011. Effect of particle size on arsenic bioaccessibility in gold mine tailings of Nova Scotia. Sci. Total Environ. 409, 2233–2243.
Meza-Figueroa, D., Maier, R.M., de la O-Villanueva, M., Gomez-Alvarez, A., Moreno-Zazueta, A., Rivera, J., et al., 2009. The impact of unconfined mine tailings in residential areas from a mining town in a semi-arid environment: Nacozari, Sonora, Mexico. Chemosphere 77, 140–147.
Nordstrom, D.K., Alpers, C.N., 1999. Negative pH, efflorescent mineralogy, and consequences for environmental restoration at the Iron Mountain Superfund site, California. Proc. Natl. Acad. Sci. 96, 3455–3462.
Offer, Z.Y., Goossens, D., 2001. Ten years of aeolian dust dynamics in a desert region (Negev desert, Israel): analysis of airborne dust concentration, dust accumulation and the high-magnitude dust events. J. Arid Environ. 47, 211–249.
Offer, Z.Y., Goossens, D., 2004. Thirteen years of aeolian dust dynamics in a desert region (Negev desert, Israel): analysis of horizontal and vertical dust flux, vertical dust distribution and dust grain size. J. Arid Environ. 57, 117.
Paktunc, D., Bruggeman, K., 2010. Solubility of nanocrystalline scorodite and amorphous ferric arsenate: implications for stabilization of arsenic in mine wastes. Appl. Geochem. 25, 674–683.
Paktunc, D., Dutrizac, J., Gertsman, V., 2008. Synthesis and phase transformations involving scorodite, ferric arsenate and arsenical ferrihydrite: implications for arsenic mobility. Geochim. Cosmochim. Acta 72, 2649–2672.
Plumlee, G.S., Ziegler, T.L., 2003. The medical geochemistry of dusts, soils, and other earth materials. Treatise on Geochemistry. Environmental Geochemistry 9, 263–310.
Proffitt, A.P.B., Rose, C.W., Hairsine, P.B., 1991. Rainfall detachment and deposition-experiments with low slopes and significant water depths. Soil Sci. Soc. Am. J. 55, 325–332.
Reeder, R.J., Schoonen, M.A.A., Lanzirotti, A., 2006. Metal speciation and its role in bioaccessibility and bioavailability. Medical Mineraology and Geochemistry 64, 59–113.
Rieuwerts, J.S., Searle, P., Buck, R., 2006. Bioaccessible arsenic in the home environment in southwest England. Sci. Total Environ. 371, 89–98.
Shaoping, H., Xincai, C., Jiyan, S., Yingxu, C., Qi, L., 2008. Particle-facilitated lead and arsenic transport in abandoned mine sites soil influenced by simulated acid rain. Chemosphere 71, 2091–2097.
Smith, D.B., Cannon, W.F., Woodruff, L.G., Solano, F., Kilburn, J.E., Fey, D.L., 2013. Geochemical and Mineralogical Data for Soils of the Conterminous United States: U.S. Geological Survey Data Series. 801.
Sobron, P., Sanz, A., Acosta, T., Rull, F., 2009. A Raman spectral study of stream waters and efflorescent salts in Rio Tinto, Spain. Spectrochimica Acta Part a-Molecular and Biomolecular Spectroscopy 71, 1678–1682.
Tchounwou, P.B., Patlolla, A.K., Centeno, J.A., 2003. Carcinogenic and systemic health effects associated with arsenic exposure—a critical review. Toxicol. Pathol. 31, 575–588.
Toujaguez, R., Ono, F.B., Martins, V., Cabrera, P.P., Blanco, A.V., Bundschuh, J., et al., 2013. Arsenic bioaccessibility in gold mine tailings of Delita, Cuba. J. Hazard. Mater. 262, 1004–1013.
USEPA, 2001. In: Agency USEP (Ed.), Technical Fact Sheet: Final Rule for Arsenic in Drinking Water. Office o Water.
USEPA, 2017. Update for Chapter 5 of the Exposure Factors Handbook, Washington D.C..
Valente, T., Grande, J.A., de la Torre, M.L., Santisteban, M., Ceron, J.C., 2013. Mineralogy and environmental relevance of AMD-precipitates from the Tharsis mines, Iberian Pyrite Belt (SW, Spain). Appl. Geochem. 39, 11–25.
Wanielista, M.P., Yousef, Y.A., 1993. Stormwater Management. John Wiley and Sons, Inc., NY, USA.
Webb, S.M., 2005. SIXpack: a graphical user interface for XAS analysis using IFEFFIT. Phys. Scr. T115, 1011–1014.
Whitacre, S., Basta, N., Stevens, B., Hanley, V., Anderson, R., Scheckel, K., 2017. Modification of an existing in vitro method to predict relative bioavailable arsenic in soils. Chemosphere 180, 545–552.
Yu, H.-Y., Liu, C., Zhu, J., Li, F., Deng, D.-M., Wang, Q., et al., 2016. Cadmium availability in rice paddy fields from a mining area: the effects of soil properties highlighting iron fractions and pH value. Environ. Pollut. 209, 38–45.

SUPPORTING INFORMATION

Wetting/drying cycles increase arsenic bioaccessibility in mine-impacted sediments

Kevan P. O'Connor[1], Michaela Montgomery[1], Randy A. Rosales[1], Katherine K. Whiteman[1], and Christopher S. Kim[1]*

[1]Schmid College of Science and Technology

Chapman University, One University Drive, Orange, CA 92866

*contact email: cskim@chapman.edu

FIGURE CAPTIONS

Figure S1. Satellite image of the Red Hill Mercury Mine and surrounding community (inset map of California shows the location of the mine). All undeveloped land in the image is part of the Red Hill Mine. Driveway location for rainwater runoff and transported sediment is indicated in the lower left-hand corner, while the in-place mine waste sampling location is indicated in the upper right-hand section of the image.

Figure S2. Photograph of Red Hill driveway sampling location during a rain event on 02/28/2014 demonstrating the channeling of rainfall runoff with visibly suspended sediment from the mine site (background) towards the publicly accessible street below (foreground).

Figure S3. Arsenic concentration of the ingestible size fraction (≤250 microns) of transported mine sediments as a function of cumulative rainfall in the 5-day period preceding sample collection *(P*=0.005*).*

Figure S4. Arsenic released in a simulated gastric fluid extraction of the ingestible size fraction (≤250 μm particle diameter) of a deposited Red Hill Mine sediment and background sample (both collected 3/3/14) as a function of post-rinse drying time. *P*=0.019 (unrinsed compared with 7 days), 0.024 (unrinsed compared with 0 days), and >0.05 (all others).

Figure S5. EXAFS spectra data and linear combination fit for Red Hill Mine site and transported sediment samples.

TABLE CAPTIONS

Table S1. Total and filtered (to 0.45 μm) arsenic concentrations of rainwater runoff samples.

Table S2. Arsenic concentration and bioaccessibility for collected Red Hill and background sediment samples. *sample not collected/analyzed.

Table S3. Effects of simulated rainwater exposure on *in vitro* arsenic bioaccessibility (IVBA) in the ingestible size fraction (≤250 μm particle diameter) of transported sediments.

Table S4. Arsenic speciation results from linear combination fitting of EXAFS spectra, for selected Red Hill samples pre- and post-simulated gastric fluid extraction, displayed in percentage and mass formats.

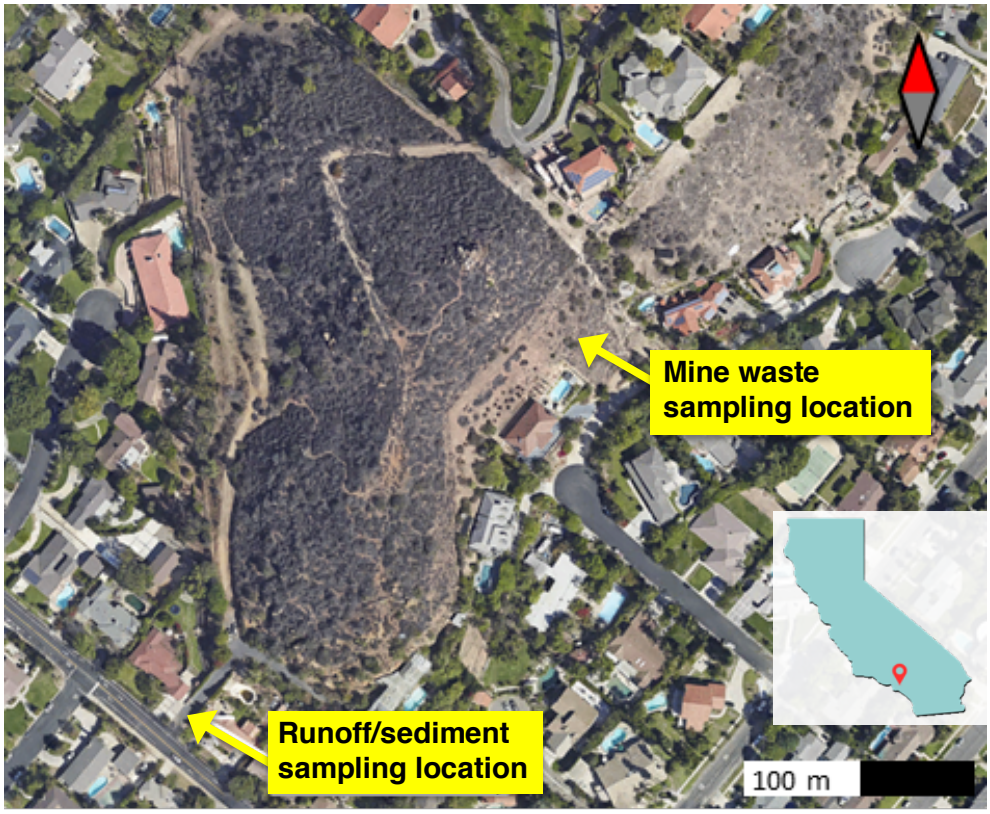
Mine waste
sampling location
Runoff/sediment
sampling location
100 m

Figure S1.

Figure S2.

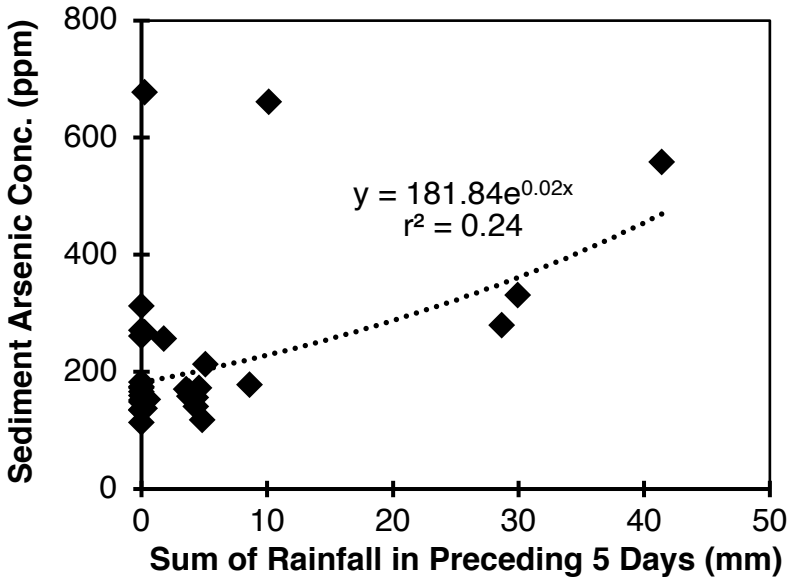
Sediment Arsenic Conc. (ppm)
800
600
400
200
0
y = 181.84e0.02x
r² = 0.24
0
10
20
30
40
50
Sum of Rainfall in Preceding 5 Days (mm)

Figure S3.

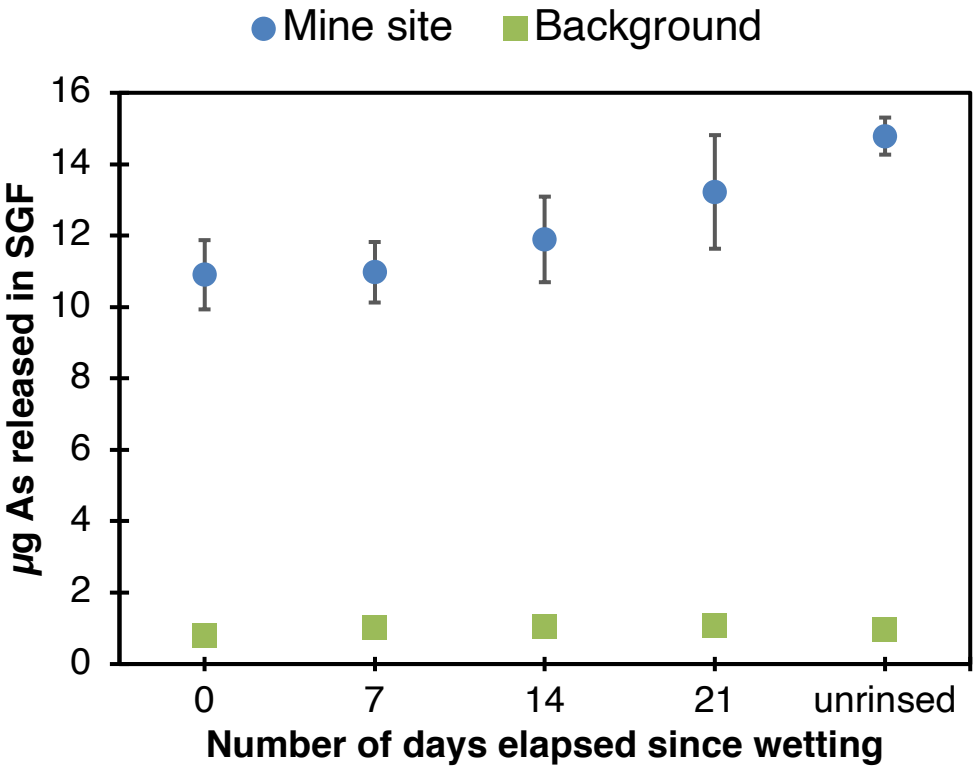
Mine site
Background
16
14
12
10
8
6
4
2
0
µg As released in SGF
0
7
14
21
unrinsed
Number of days elapsed since wetting

Figure S4.

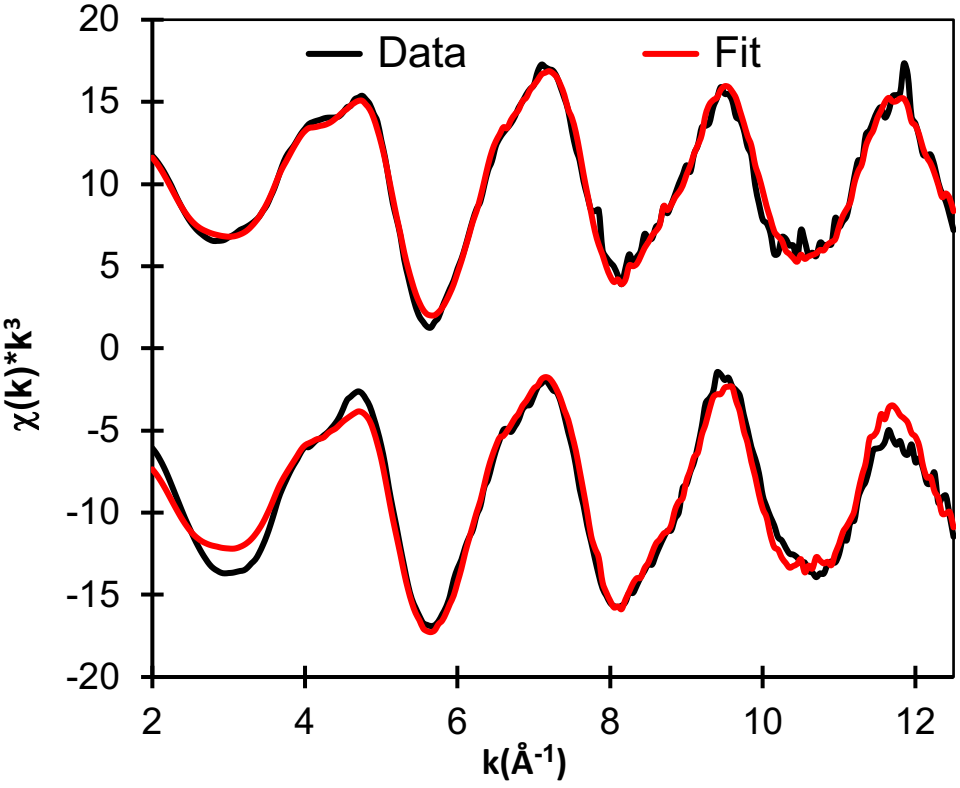

Mine Site

57% ferric arsenate
33% As(V) sorbed to iron oxyhydroxides

R-factor: 0.034

Transported Sediment

65% ferric arsenate
37% As(V) sorbed to iron oxyhydroxides

R-factor: 0.029

Figure S5.

Table S1.

Date of Collection	Location	Approximate Time of Collection	Rainfall Rate (mm/hr)	Total Arsenic Conc. (μg/L)	Filtered Arsenic Conc. (μg/L)
12/12/2009	Red Hill Driveway	12:00 PM	3.0	47.3	35.9
1/18/2010	Red Hill Driveway	11:00 PM	2.0	79.1	57.7
1/19/2010	Red Hill Driveway	2:45 PM	9.9	91.2	63.8
1/20/2010	Red Hill Driveway	4:15 PM	15.0	136	116
1/21/2010	Red Hill Driveway	1:00 PM	40.9	119	38.5
1/22/2010	Red Hill Driveway	1:15 PM	42.9	240	107
2/9/2010	Red Hill Driveway	4:00 PM	4.1	125	24.4
10/19/2010	Red Hill Driveway	3:30 PM	6.1	530.8	505.7
10/20/2010	Red Hill Driveway	4:30 PM	6.1	77.7	78.9
12/20/2010	Red Hill Driveway	4:40 PM	4.1	106	119
12/21/2010	Red Hill Driveway	8:20 PM	4.1	318	313
9/6/2011	Red Hill Driveway	3:45 PM	N/A	91.1	32.7
11/20/2011	Red Hill Driveway	5:00 PM	9.9	65.5	59.9
1/23/2012	Red Hill Driveway	11:35 AM	N/A	95.9	87.9
2/15/2012	Red Hill Driveway	6:00 PM	0.3	33.3	23.1
11/30/2012	Red Hill Driveway	12:30 PM	0.3	130	100
1/25/2013	Red Hill Driveway	8:00 AM	0.3	36	33
12/2/2014	Red Hill Driveway	12:15 PM	1.0	380	270
12/12/2014	Red Hill Driveway	11:00 AM	9.9	350	390
12/12/2014	Red Hill Driveway	11:45 AM	1.0	390	310
1/11/2015	Red Hill Driveway	9:05 AM	5.3	90	55
12/20/2010	Background Site	4:40 PM	4.1	9.1	5.1
3/20/2011	Background Site	7:10 PM	2.0	<1	<1
9/6/2011	Background Site	3:45 PM	N/A	<1	1.6
11/20/2011	Background Site	2:15 PM	N/A	3.7	3.9
11/20/2011	Background Site	2:15 PM	N/A	3.7	3.9
11/20/2011	Background Site	5:00 PM	9.9	1.2	<1
1/23/2012	Background Site	11:35 AM	N/A	<1	1.2
2/15/2012	Background Site	6:00 PM	0.3	1.4	<1
11/30/2012	Background Site	1:00 PM	0.3	<10	<10
1/25/2013	Background Site	8:30 AM	0.3	<10	<10
12/2/2014	Background Site	12:00 PM	1.0	<1	<1
12/12/2014	Background Site	10:45 AM	9.9	<1	<1

Table S2.

	Red Hill Sediment					Background Sediment	
Collection Date	As Conc. of Ingestible Size Fraction (mg/kg)	As Conc. of Bulk Sample (mg/kg)	Ingestible Fraction/Bulk (% Enrichment)	As Bioaccessibility (%)	Std Dev	As Conc. of Ingestible Size Fraction (mg/kg)	As Conc. of Bulk Sample (mg/kg)
1/4/2013	213	163	31%	4.1%	0.41%	8	4
2/4/2013	183	127	44%	6.8%	0.77%	<5	5
2/11/2013	173	143	21%	7.4%	0.68%	<5	4
2/20/2013	171	135	27%	8.5%	0.22%	<5	4
3/4/2013	173	102	70%	7.8%	0.47%	<5	4
4/1/2013	178	97	84%	6.8%	0.44%	8	6
5/7/2013	118	34.8	239%	14.7%	0.41%	5.3	3.8
6/5/2013	153	86.3	77%	8.0%	0.12%	6	4.4
7/8/2013	114	56.4	101%	10.3%	0.43%	5.6	4.6
8/5/2013	175	68	157%	21.8%	0.15%	9	9
9/9/2013	166	63	163%	19.1%	0.22%	16	10
10/7/2013	160	28	471%	20.1%	1.63%	12	13
10/10/2013	157	57	175%	12.2%	0.34%	13	4
10/29/2013	153	47	226%	15.4%	0.22%	10	8
11/4/2013	135	38	255%	18.2%	0.15%	11	10
11/25/2013	166	54	207%	21.6%	1.31%	12	6
12/2/2013	141	143	-1%	15.9%	0.80%	11	6
12/22/2013	159	64	148%	15.1%	0.21%	9	9
1/6/2014	149	52	187%	13.2%	0.18%	10	7
2/3/2014	138	60	130%	24.9%	1.45%	5	5
2/25/2014	136	27	404%	18.4%	0.15%	8	5
3/3/2014	559	475	18%	4.6%	0.29%	<5	4
3/3/2014	449	410	10%	3.3%	0.21%	*	*
4/2/2014	257	93	176%	6.8%	0.21%	<5	27
5/1/2014	268	153	75%	10.9%	0.17%	<5	11
7/7/2014	271	156	74%	11.8%	0.85%	*	*
8/1/2014	313	134	134%	9.7%	0.55%	*	*
11/2/2014	662	567	17%	2.7%	0.04%	17	31
12/1/2014	678	365	86%	4.5%	0.03%	17	26
12/4/2014	331	211	57%	5.3%	0.31%	16	10
1/6/2015	261	193	35%	5.2%	0.16%	*	*
1/12/2015	280	133	111%	3.1%	0.09%	*	*
Min	114	27	-1%	2.7%	0.03%	5	4
Max	678	567	471%	24.9%	1.63%	17	31
Avg.	239	142	125%	11.2%	0.43%	10	9
Std. Dev.	149	132	109%	6.3%	0.40%	4	7

Table S3.

Date of Collection	As Conc. (mg/kg)	Preceding dry days	Unrinsed IVBA	Std. Dev.	Rinsed IVBA	Std. Dev.	Absolute Change in IVBA	% Change in IVBA
8/5/13	175	9	20.4%	0.4%	17.5%	0.3%	-2.9%	-14%
2/25/14	136	17	18.7%	0.5%	15.0%	0.2%	-3.7%	-20%
5/7/13	118	0	13.2%	0.6%	11.5%	0.5%	-1.7%	-13%
7/7/14	271	73	10.7%	0.1%	6.5%	0.3%	-4.1%	-39%
3/3/14	559	0	4.6%	0.1%	3.3%	0.1%	-1.3%	-28%

Table S4.

				As(V) sorbed to goethite		Scorodite		Sodium arsenate	
Collection Date	**IVBA %**	**Description**	**[As] (mg/kg)**	**EXAFS proportion**	**As mass (per kg sample)**	**EXAFS proportion**	**As mass (per kg sample)**	**EXAFS proportion**	**As mass (per kg sample)**
8/5/13	21.8%	Pre-Extraction	175	59%	103	15%	26	32%	56
		Post-Extraction	137	56%	77	5%	7	46%	63
		% Difference			**-26%**		**-74%**		**12%**
10/7/13	20.1%	Pre-Extraction	160	45%	72	38%	61	18%	29
		Post-Extraction	128	49%	63	30%	38	30%	38
		% Difference			**-13%**		**-37%**		**33%**
2/25/14	18.4%	Pre-Extraction	136	37%	50	33%	45	36%	49
		Post-Extraction	111	45%	50	13%	14	48%	53
		% Difference			**-1%**		**-68%**		**9%**
11/4/13	18.2%	Pre-Extraction	135	62%	84	0%	0	63%	85
		Post-Extraction	110	62%	68	0%	0	56%	62
		% Difference			**-18%**		**-**		**-27%**
7/7/14	11.8%	Pre-Extraction	271	30%	81	42%	114	28%	76
		Post-Extraction	239	53%	127	29%	69	4%	10
		% Difference			**56%**		**-39%**		**-87%**

Table S4 (continued).

				As(V) sorbed to goethite		Scorodite		Sodium arsenate	
Collection Date	**IVBA %**	**Description**	**[As] (mg/kg)**	**EXAFS proportion**	**As mass (per kg sample)**	**EXAFS proportion**	**As mass (per kg sample)**	**EXAFS proportion**	**As mass (per kg sample)**
7/8/14	10.3%	Pre-Extraction	114	46%	52	18%	21	36%	41
		Post-Extraction	102	46%	47	14%	14	53%	54
		% Difference			**-10%**		**-30%**		**32%**
2/4/13	6.8%	Pre-Extraction	183	28%	51	22%	40	44%	81
		Post-Extraction	171	27%	46	28%	48	28%	48
		% Difference			**-10%**		**19%**		**-41%**
3/3/14	4.6%	Pre-Extraction	559	41%	229	38%	212	23%	129
		Post-Extraction	533	54%	288	39%	208	0%	0
		% Difference			**26%**		**-2%**		**-100%**